EUROPEAN ORGANIZATION FOR NUCLEAR RESEARCH

PH I/COM-70/57
30 November, 1970

PHYSICS I
ELECTRONICS EXPERIMENTS COMMITTEE

Addendum to
A proposal to study the production of cascade particles from K^-p interactions

by

T.A. Broome, J.K. Davies, B.G. Duff, R.C. Hanna,
D.C. Imrie, G.J. Lush, D.R. Quarrie,
L.A. Robbins, E.J. Sacharides,
A.D. Smith, D.H. White
and E.G. Xereas
(University College London-Rutherford High Energy Laboratory)

INTRODUCTION

During the course of the last six months, detailed work has been carried out on the various measurements which can be made on cascade states using the equipment described in the main proposal. In addition, a number of useful discussions have taken place at C.E.R.N., and as a result, we would like to present this addendum which discusses the following topics:

A) The priorities of the experimental programme,

B) Choice of beam characteristics,

and C) Revised estimates of event rates and running times,

together with a short appendix on the comparison of the proposed method with recent bubble chamber and Omega project proposals.

A) The Priorities of the Experimental Programme

1) Statement of Aims

The main object of the experiment is to look for excited cascade states in a mass region from 1750 to 2350 MeV and to confirm the existence of the states so far proposed. We note that the region around 1820 MeV is confused and that states probably exist near 1930, 2030 and 2240 MeV.

First, a missing mass search will be carried out at several momenta (see section B) in order to help in the removal of kinematic reflections, and also to help in the optimisation of the production of different cascade mass regions. Next, the events recorded on magnetic tape will be analysed in order to extract a sample of clear examples of certain decay modes (see below). The branching ratios thus obtained, after various corrections have been applied, will be useful in making assignments of I, J and P for the observed excited states. Finally, the decay distributions for these decay modes will be analysed to assist in making J and P assignments.

In principle, a study of the production angular distributions of the cascade states yields information on Y^* exchanges at low incident energies, and Regge exchanges at high energies. However, experimentally these are difficult measurements as the efficiencies of the K^+ detectors must be known in detail as a function of angle and position. In addition, the Y^* region would require data to be taken at low momenta, and preferably at a series of closely spaced momentum intervals. These requirements are not really compatible with the high mass cascade search and therefore we do not intend to study production mechanisms in detail, although a measurement of the conjectured Regge backward peaking at high energies will be possible.

2) Cascade Spectroscopy

The missing mass analysis will be carried out in three stages:

a) During the course of the experiment, an on-line reconstruction of the "labelled" K^+ track will give the missing mass of all other final state particles, which will give rise to peaks from primary resonant states.

b) After geometric reconstruction of the event, certain topological cuts can be imposed on the sample given in a). For example, it will be possible to insist that the total number of charged particles be appropriate, and to require a second vertex (corresponding to a Λ decay). Thus, the sample given in a) would be reduced to the "serious candidates".

c) The sample of events selected by b) would then be tested for momentum and energy balance in order to select events which contain 4 or 6 charged particles together with 0 or 1 uncharged particle. Monte Carlo calculations indicate that it will be possible to distinguish cleanly between events in which all particles are observed, or ones in which there is only one missing neutral, or where there is more than one missing neutral.

Events in which all final state particles are observed or ones in which there is only one missing neutral can then be tested for one of the particular decay modes discussed in the next section. This final missing mass spectrum will then contain only those events which satisfactorily fit one of these decay modes.

The missing mass resolution has been studied using Monte Carlo methods and is predicted to be approximately $\pm$ 15 MeV. This resolution is in fact a function of the incident momentum and the missing particle and the value quoted is only a typical value. To obtain this figure, it has been assumed that the sagitta of a curved track can be determined to $\pm \frac{1}{2}$ mm and that the beam momentum resolution is $\pm \frac{1}{2}\%$.

3) Branching Ratios

For simplicity, consider the decay of a charged excited cascade state produced in association with a K^+. (A similar analysis to the one below has also been carried out for neutral cascades, and also for production with a K^* (890)). The main decay modes are shown in Table 1, and in the same table the particular final states are indicated which correspond to the prescription for "clean" events discussed in the previous section. The acceptances for these final states have also been estimated using Monte Carlo methods. As an example column c) of Table 1 shows that for a Ξ^* with a mass of 2030 MeV and an incident beam momentum of 3.5 GeV/c, the acceptance for the 6 modes varies from 30% to 50% . Generally, the whole decay angular distribution will be observed with a reasonable efficiency. As an example. Figure 1 shows the acceptance for channel (2) AND (4) as a function of the decay angle in the centre of mass, where an isotropic decay distribution has been assumed.

From these considerations, it should be possible to estimate branching ratios for $\Xi\pi : \Xi^*(1530)\pi : \Lambda\bar{K} : \Sigma\bar{K}$, with the usual problem that there will be mixing in the $\Lambda\bar{K}$ and $\Sigma\bar{K}$ channels. However, a clean sample of $\Sigma^-\bar{K}^0$ decays should assist in the separation from simple isotopic spin arguments.

In particular, it should be possible to measure the ratio $\Xi^0\pi^-/\Xi^-\pi^0$ with little bias, as the same final state particles are involved in both modes. Thus, whenever, the $(\Xi\pi)$ decay mode is observed there will be the possibility to check that $I=\frac{1}{2}$ for the Ξ^*, as the ratio is predicted to be $\frac{1}{2}$ if I=3/2 or 2 if I=1/2. (A similar check will also be available from the decay of neutral excited cascades into $(\Xi^-\pi^0)\pi^+$ or $(\Xi^-\pi^+)\pi^0$ from the $(\Xi^*(1530)\pi)$ decay mode. The ratio $(\Xi^-\pi^0)\pi^+/(\Xi^-\pi^+)\pi^0$ is predicted to be 4 for I=3/2 and 1 for 1/2 respectively.)

TABLE I PRINCIPAL DECAY MODES OF CHARGED Ξ RESONANCES

DECAY MODE	CHARGED MODE	(C-G COEFFS)^2 FOR Ξ^* WITH $I=\frac{1}{2}$	$I=\frac{3}{2}$	CHANNEL NO.	FINAL STATE OBSERVED 'CLEANLY'	FRACTION OF TOTAL DECAY MODE OBSERVED DUE TO:– i ISOSPIN [a]	ii WEAK DECAY OF $\Lambda, \Sigma, \bar{K}^0$	iii SPARK CHAMB. ACCEPTANCE [b]
$(\Xi\pi)$	$\Xi^0\pi^-$	$\frac{2}{3}$	$\frac{1}{3}$	1	$(\Lambda\pi^0)\pi^- \to (\pi^- p)\pi^0\pi^-$	$\frac{2}{3}$	0.65	0.43
	$\Xi^-\pi^0$	$\frac{1}{3}$	$\frac{2}{3}$	2	$(\Lambda\pi^-)\pi^0 \to (\pi^- p)\pi^-\pi^0$	$\frac{1}{3}$	0.65	0.50
$(\Xi^*(1530)\pi) \hookrightarrow \Xi\pi$ [c]	$(\Xi^-\pi^+)\pi^-$	$\frac{4}{9}$	$\frac{2}{9}$	3	$(\Lambda\pi^-)\pi^+\pi^- \to (\pi^- p)\pi^-\pi^+\pi^-$	$\frac{4}{9}$	0.65	0.30
	$(\Xi^0\pi^0)\pi^-$	$\frac{2}{9}$	$\frac{1}{9}$					
	$(\Xi^-\pi^0)\pi^0$	$\frac{1}{9}$	$\frac{2}{9}$					
	$(\Xi^0\pi^-)\pi^0$	$\frac{2}{9}$	$\frac{4}{9}$					
(ΛK^-)	ΛK^-	1	0	4	$(\pi^- p)K^-$	1	0.65	0.51
$(\Sigma\bar{K})$	$\Sigma^0 K^-$	$\frac{1}{3}$	$\frac{2}{3}$	5	$(\Lambda\gamma)K^- \to (\pi^- p)\gamma K^-$ [d]	$\frac{1}{3}$	0.65	0.51
	$\Sigma^-\bar{K}^0$	$\frac{2}{3}$	$\frac{1}{3}$	6	$\Sigma^- K^S_0 \to (\pi^- n)(\pi^+\pi^-)$	$\frac{2}{3}$	$(1)(\frac{1}{2})(0.69)$	0.30

a ASSUMING $I = \frac{1}{2}$.

b FIGURES GIVEN FOR A Ξ^* MASS OF 2030 MeV/c^2 AND AN INCIDENT K^- MOMENTUM OF 3.5 GeV/c USING CRITERIA DISCUSSED IN THE TEXT.

c HERE WE ASSUME ISOSPIN OF $\Xi^*(1530) = \frac{1}{2}$.

d IT WILL ONLY BE POSSIBLE TO CARRY OUT A VERY LIMITED SEPARATION OF ΛK^- AND $\Sigma^0 K^-$.

An SU(3) model can be used to make use of the branching ratio information to help assign an excited cascade state to a particular J,P multiplet. It can be assumed that the partial width, Γ, for a member of an SU(3) multiplet decaying into a member of the $\frac{1}{2}^+$ baryon octet and a member of the 0^- meson octet is of the form:

$$\Gamma = C^2 \, |M|^2 \, B_\ell \, (p)(p/m)$$

where p is the centre of mass momentum of one of the decay particles, m is the mass of the resonance, B_ℓ is a barrier penetration factor for angular momentum $|M|^2$ is the effective matrix element and C is the appropriate SU(3) Clebsch-Gordan coefficient. The matrix element can be estimated by fitting all the data on transitions by members of well-established multiplets to the ground state octet members (excluding the excited cascade particles). It is thus possible to predict the partial widths for $\Xi\pi$, $\Lambda\bar{K}$, and $\Sigma\bar{K}$ decay modes for the excited cascade states of the well-established multiplets. Such an analysis has recently been carried out[(1)] and the predictions are given in Table 2.

It is not yet possible to predict the partial width of the $(\Xi^*(1530)\pi)$ mode, as this would require knowledge of the coupling of the various multiplets with the $3/2^+$ baryon decuplet and such information is at present very sparse.

With the aid of such an SU(3) analysis, the determination of the mass of an excited cascade together with primary branching ratios gives vital information on the assignment of J^P for that state. It is worth remarking that even if it proves to be impossible to carry out any separation of the $\Lambda\bar{K}$ and $\Sigma\bar{K}$ channels, the ratio $\Xi\pi/(\Lambda\bar{K}+\Sigma\bar{K})$ is predicted to be very different for the various multiplets. (See Table 2).

TABLE 2 PREDICTED Ξ RESONANCES.

MULTIPLET	MASS (MeV)	DECAY MODE	PARTIAL WIDTH (MeV)	RATIOS OF PARTIAL WIDTHS $\frac{\Xi\pi}{\Lambda\bar{K}+\Sigma\bar{K}}$
$\frac{7}{2}^+$ DECUPLET	2160			
		$\Xi\pi$	21	0.51
		$\Sigma\bar{K}$	15	
		$\Xi\eta$	3	
		$\Lambda\bar{K}$	26	
$\frac{5}{2}^-$ OCTET	1950			
		$\Xi\pi$	70	2.2
		$\Sigma\bar{K}$	18	
		$\Xi\eta$	0	
		$\Lambda\bar{K}$	14	
$\frac{5}{2}^+$ OCTET	1985			
		$\Xi\pi$	0	0
		$\Sigma\bar{K}$	26	
		$\Xi\eta$	0	
		$\Lambda\bar{K}$	5	
$\frac{1}{2}^-$ NONET	1825			
		$\Xi\pi$	62	0.64
		$\Sigma\bar{K}$	17	
		$\Lambda\bar{K}$	80	
$\frac{3}{2}^-$ NONET	1800			
		$\Xi\pi$	4	0.33
		$\Sigma\bar{K}$	5	
		$\Lambda\bar{K}$	7	

4) Decay Angular Distributions

All decay modes observed in the experiment will be of the type:

Spin J $\rightarrow$ Spin $\frac{1}{2}$ + Spin 0

Or Spin J $\rightarrow$ Spin 3/2 + Spin 0

The method of analysis used by Byers and Fenster(2) and modified by Button-Shafer(3) for the spin 3/2 case, gives a best fit J^P assignment using a maximum likelihood technique.

As has been discussed above, the acceptance of the equipment is such that a full coverage of the decay distributions will be obtained, and provided that the backgrounds are not too large, a decay analysis should give useful information on J^P assignments.

B) Choice of Beam Characteristics

1) Beam Momenta

The following factors will affect the choice of beam momenta:

a) Production Cross-section and Phase Space

For any given mass state, it is necessary to be sufficiently far above threshold to provide a reasonable phase space for the production of that state. As a guide, the total cross-section for the ground state production as a function of the centre of mass momentum (p) of the outgoing K^+ has been fitted according to:

$$\sigma = 3\, X_{max}\, p^4_{max} \cdot p^2/(p^6 + 2p^6_{max})$$

where X_{max} is the maximum total cross-section and p_{max} the corresponding momentum. This "model" assumes that production is dominated by threshold phase-space behaviour and a fall-off of p^{-4} at high momenta. The value of p_{max} for this ground state case is 0.45 GeV/c and it is guessed that this number is universal for high mass states. On this assumption, as an example, Figure 2 shows the predicted shape for the production cross-section for the $\Xi^*(2030)$ as a function of incident momentum. It will be noted that the peak occurs at 3.4 GeV/c whereas the threshold is at 2.8 GeV/c.

b) K^+ Detector Acceptance

The upper limit for momentum accepted by the K^+detector is 1.0 GeV/c (see main proposal paper). As the beam momentum is increased, the kinematics are such that this limit cuts further and further towards the backward direction. Again using Ξ^* (2030) as an example, Figure 3 shows how much of the cos θ cm production is lost as the incident momentum is increased from 2.8 to 4.6 GeV/c. It can also be seen that as the incident momentum increases, even for the accepted angular region, the K^+ laboratory angle increases and this leads to a loss of azimuthal acceptance.

The combined effects of a) and b) have been estimated in a Monte Carlo programme which includes the geometry of the target and the detectors, the trajectories in the magnetic field, K^+ decays in flight and normalization to a cross-section given by the above prescription. Two cases have been considered. First, in which the production differential cross-section is taken as flat in the cosine of the centre of mass angle, and secondly for a production going as $e^{3.4\ u}$(which is the backward peaking observed in the ground state production). In fact, the evidence from high energy experiments suggests that the distributions for the high mass states will be somewhere between these extremes. The results are shown in Figure 4, in which the normalized acceptances are shown as a function of incident momentum for the production of the Ξ^* (2030).

The results indicate that if some backward peaking is expected, then it is reasonable to choose a momentum near to the peak for the production cross-section, as in this case with the particular geometry of detectors proposed, the effects of K^+ acceptance are not too serious. (However, for the flat distribution case it is clear that there is an advantage in working at a rather lower momentum.)

c) Spark Chamber Acceptance.

Generally, the acceptance for the various decay channels discussed above will improve with increased incoming momentum as the secondary particles are thrown forward. As a typical example, channel (2) of Table 1 has an acceptance which increases from 44% at 3.0 GeV/c to 62% at 4.0 GeV/c (where, as in Table 1 the Ξ^* (2030) is the decaying particle).

Thus, unlike the K^+ acceptance, as far as the individual decay mode acceptances are concerned, there is an advantage in working at a higher momenta.

d) Kinematic Reflections.

It is clear that it is necessary to work at several momenta in order to distinguish between genuine peaks in missing mass plots and false peaks arising from kinematic effects (e.g. from reflections of the ϕ in channels 4 and 5). On the basis of the above considerations, it would seem that data should be taken at 4 momenta at 3.0, 3.5, 4.0 and 4.5 GeV/c, in order to cover the mass states 1820, 1930, 2030 and 2240. (In the original proposal, 4 runs were suggested between 2.0 and 4.0 GeV/c). At a later stage, if it is decided to study the proposed states at 1635 and 2500 MeV, then additional momentum settings will be necessary.

2) Beam Resolution

In order to obtain the missing mass resolution quoted above, it has been assumed that it would be possible to produce a K^- beam with 0.5% resolution. In practice, it may be possible to take a larger momentum bite than this and to measure individually the momenta of the incoming particles with a precision of

0.5% or better using small proportional chambers on either side of a bending magnet in the beam. A suitable proportional chamber has been built by this group.

3)Beam Intensity

It is assumed that it will be possible to obtain 10^4 K^-'s per pulse at momenta from 3.0 to 4.5 GeV/c. Considerations of random rates in the various detecting elements suggests that an enriched beam would be desirable, but not absolutely necessary.

C) Revised Estimates of Event Rates and Running times

1)Event Rates

As an example, an estimate is given for the detection of events arising from the production of Ξ^* (2030) in the reaction $K^- + P \rightarrow \Xi^* + K^+$ with an incident K^- beam at a momentum of 3.5 GeV/c. The following data is used:

a) 50 cm Hydrogen target

b) 10,000 K^-'s / pulse

c) 30 pulses/minute (i.e. 24 GeV GeV/c internal beam with a 400 ms flat top)

d) assume an $e^{3.4\,u}$ production mechanism

e) acceptance of the K^+ detector is 15% (This factor, produced from a Monte Carlo programme, includes the geometry of the detectors, K^+ decay, and assumption d)

f) the $K\mu 2$ branching ratio is 63%

g) efficiency for detecting the decay muons is 46% (This factor includes the effect of the time gate in the detector)

These estimates then yield:

$$10^4 \cdot (6.10^{23} \cdot 50 \cdot 0.07) \cdot (0.15 \cdot 0.63 \cdot 0.46) \cdot 10^{-30} \text{ events/pulse/}\mu\text{b}$$

$$= 0.9 \cdot 10^{-3} \text{ events/pulse/}\mu\text{b}$$

= 40 events /μb / day (or 30 events/μb / day if a flat production mechanism is assumed instead of assumption d).

This number varies with incident momentum and missing mass, but this particular estimate will give a guide to the expected rates for a particular mass state which is produced near the optimum beam energy. (This estimate would be reduced by a factor of about 2 if the Ξ^* (2030) is produced at 4.5 GeV/c.)

Taking the above estimate as typical, $1\frac{1}{2}$ weeks running at each of the four momentum settings will give a gross yield

<u>1650 events / μb</u> (spread over the 4 momenta)

The data shown in Figure 2 of the main proposal suggest that the total triggering cross-section will be in the region of 150 μb. It can be estimated that about one quarter of the total cross-section will involve the production of a cascade state other than the ground state and the Ξ^* (1530). Thus, for the total running time suggested above, there will be:

$\sim$250,000 Triggers

<u>$\sim$60,000 Ξ^*'s produced</u> with a mass greater than 1530 MeV.

Table 1 shows the figures which suggest that approximately one third of the Ξ^*'s produced will decay into a final state which will be reconstructed. There will therefore be:

<u>$\sim$ 20,000 Reconstructed Ξ^* Decays</u>

(excluding the ground state and the 1530)

2) <u>Running Time Request</u>

We are requesting $1\frac{1}{2}$ useful data-taking weeks at each of the 4 momenta, 3.0, 3.5, 4.0 and 4.5 GeV/c in a beam giving 10^4 K^-'s / pulse. In addition we will require setting-up time, taking some small fraction of such a beam, for a further 4 weeks. (As was discussed in the main proposal, it is intended that the complete equipment be assembled and tested at the Rutherford Laboratory before being moved to C.E.R.N.)

REFERENCES

1) Nuc.Phys. B22, 93 (1970)

2) Phys.Rev.Letters 11, 56 (1963)

3) Phys.Rev. 139, B605 (1965)

APPENDIX (1) Comparison with Bubble Chamber and Ω Project Techniques

I BUBBLE CHAMBER

The main advantage of the proposed technique over a bubble chamber experiment is that the bulk of the events will contain a K^+ so ensuring that a strangeness change of -2 has occurred., Also, as a large flux of K^-'s can be taken, a much larger number of events can be produced in a reasonable run. Our equipment, with an estimated $\sim$1500 events / μb is to be compared with the largest bubble chamber experiment so far published at $\sim$30 events/ μb and with the largest proposal (for the 12' chamber at the Z.G.S.) that we are aware of, at $\sim$100 events / μb . The scanning and measuring problem for such a vast bubble chamber experiment will be very considerable.

Bubble chamber experiments have the same difficulty in reconstructing events with missing neutrals, and thus basically the same isotopic spin factors (given in Table 1) apply to such experiments. In addition, such experiments are by no means completely bias free, weighting of up to a factor of 2 often being applied to certain decay channels.

The Bubble Chamber technique has an advantage in missing mass resolution. In our case, this resolution will be typically $\pm$ 15 MeV (as discussed above) and for the Bubble Chamber case is typically 10 MeV. However, it should be remembered that the high mass resonances are thought to have widths which are of the order of 50 to 100 MeV.

II Ω PROJECT PROPOSAL

The physical size of the required magnetic volume for the experiment is determined by:

a) Decay paths of the low momentum K^+'s

b) Reasonable aperture sizes for the K^+ detectors

c) The solid angle for acceptance of the final state particles.

The two factors a) and b) require a magnetic volume with a cross section not much larger than 1 m X 1 m . The length of the magnetic field region which can be usefully used will depend on how much the decay particles are "thrown forward" and this will depend on the incident momentum.

For a high momentum run, there will certainly be an advantage in using a magnet of the size under construction for the Ω project. Such increased track lengths will also improve the missing mass resolution. However, for lower incident momenta (say up to $\sim$ 4 GeV/c) there is very little to be gained.

We also feel that a comparatively complex triggering arrangement of the type we are proposing would require the magnet for a time which may well not be compatible with a piece of equipment required for use by a large number of groups.

However, the high momentum proposal from the Imperial College group would form a natural extension of our proposed experiment and will certainly provide information on the very high mass resonance region barely covered by our proposal.

APPENDIX 2

Personnel

The following members of the UCL/RHEL collaboration are currently involved with this proposal.

UCL

Staff:	Dr B.G. Duff
	Dr D.C. Imrie
	Dr G.J. Lush
	Mr L.A. Robbins
	Dr A.D. Smith
	Prof DH White
Technical Staff :	Mr D.B. Webb
	Mr H. Bhunnoo
Research Students :	Mr T.A. Broome
	Mr J.K. Davies
	Mr E.G. Xereas
	Mr D.R. Quarrie

RHEL

Staff:	Dr R.C. Hanna
	Dr E.J. Sacharides

Figure 1 RELATIVE DETECTION EFFICIENCY VERSUS Ξ^* (2030) DECAY ANGLE FOR Ξ^* (2030) $\longrightarrow \Xi$ (1320) π AND Ξ^* (2030) $\longrightarrow \Lambda K^-$

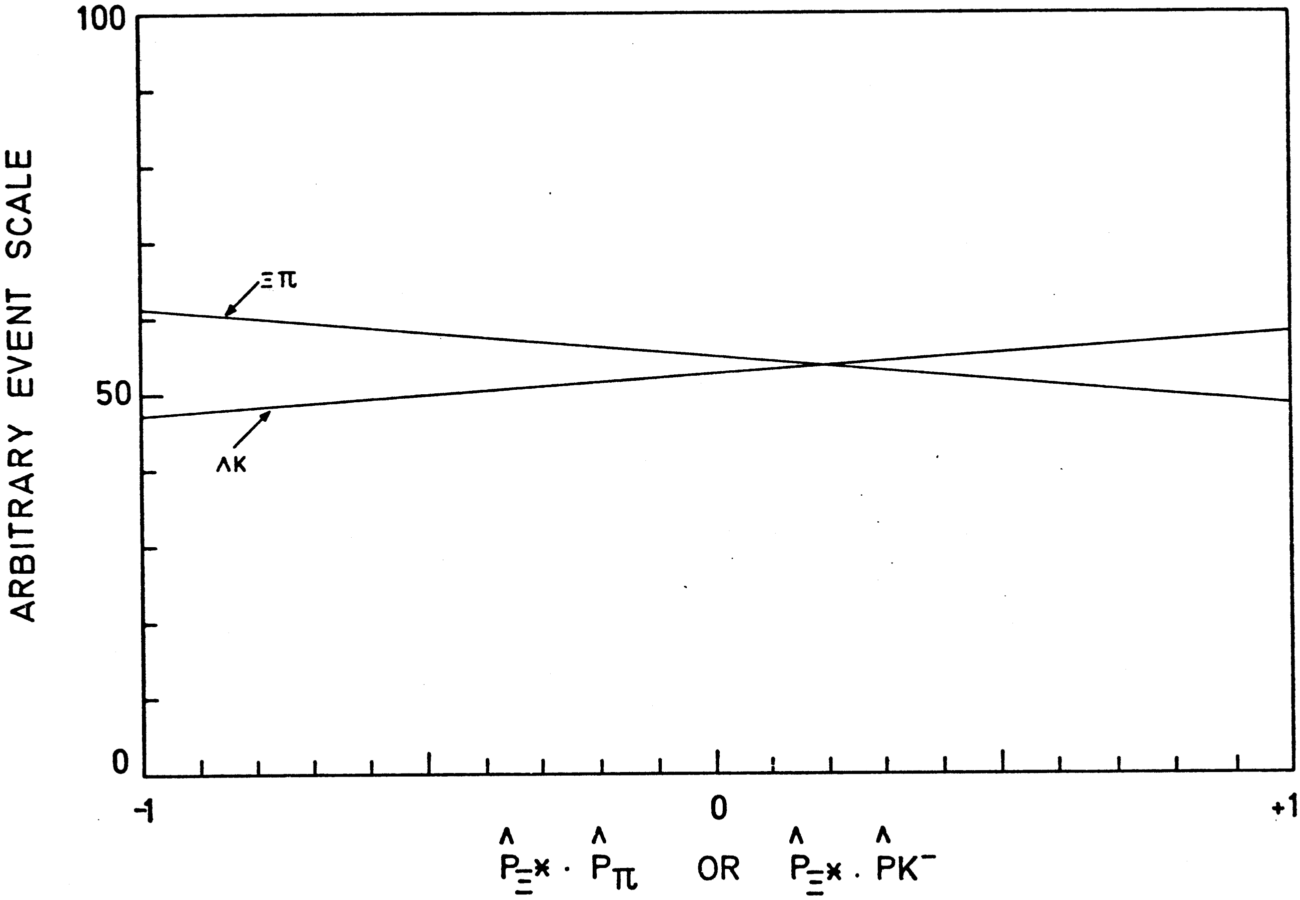

Figure 2 PERCENTAGE OF MAXIMUM CROSS SECTION VERSUS INCIDENT MOMENTUM

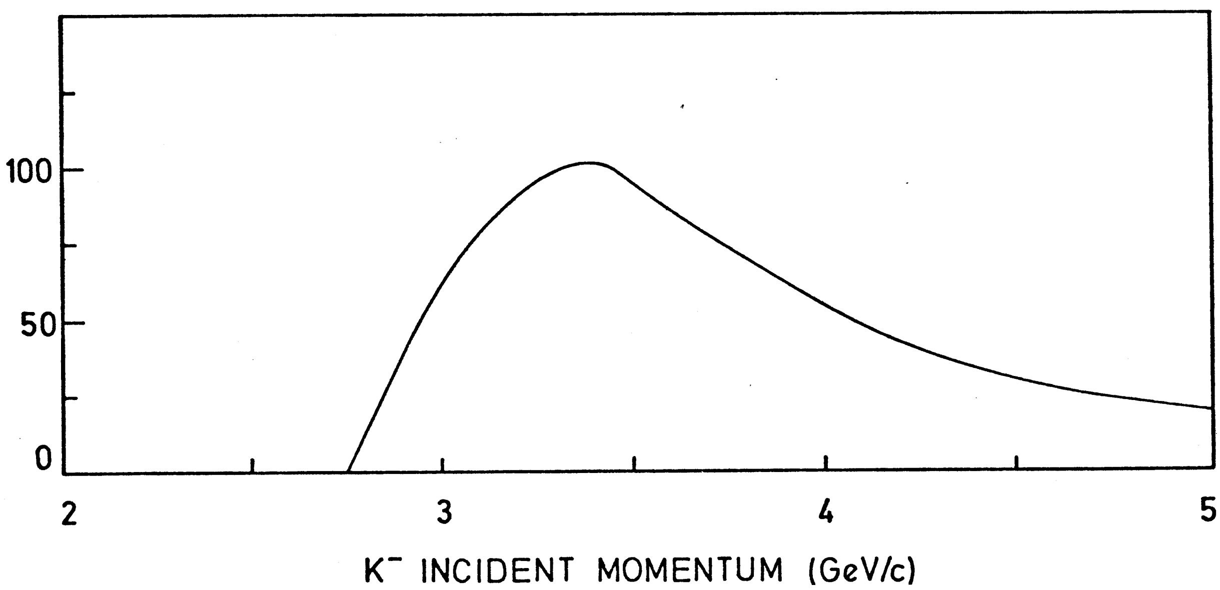

Figure 3 KINEMATIC CURVES FOR $K^- + PROTON \rightarrow K^+ + \Xi(2030)$

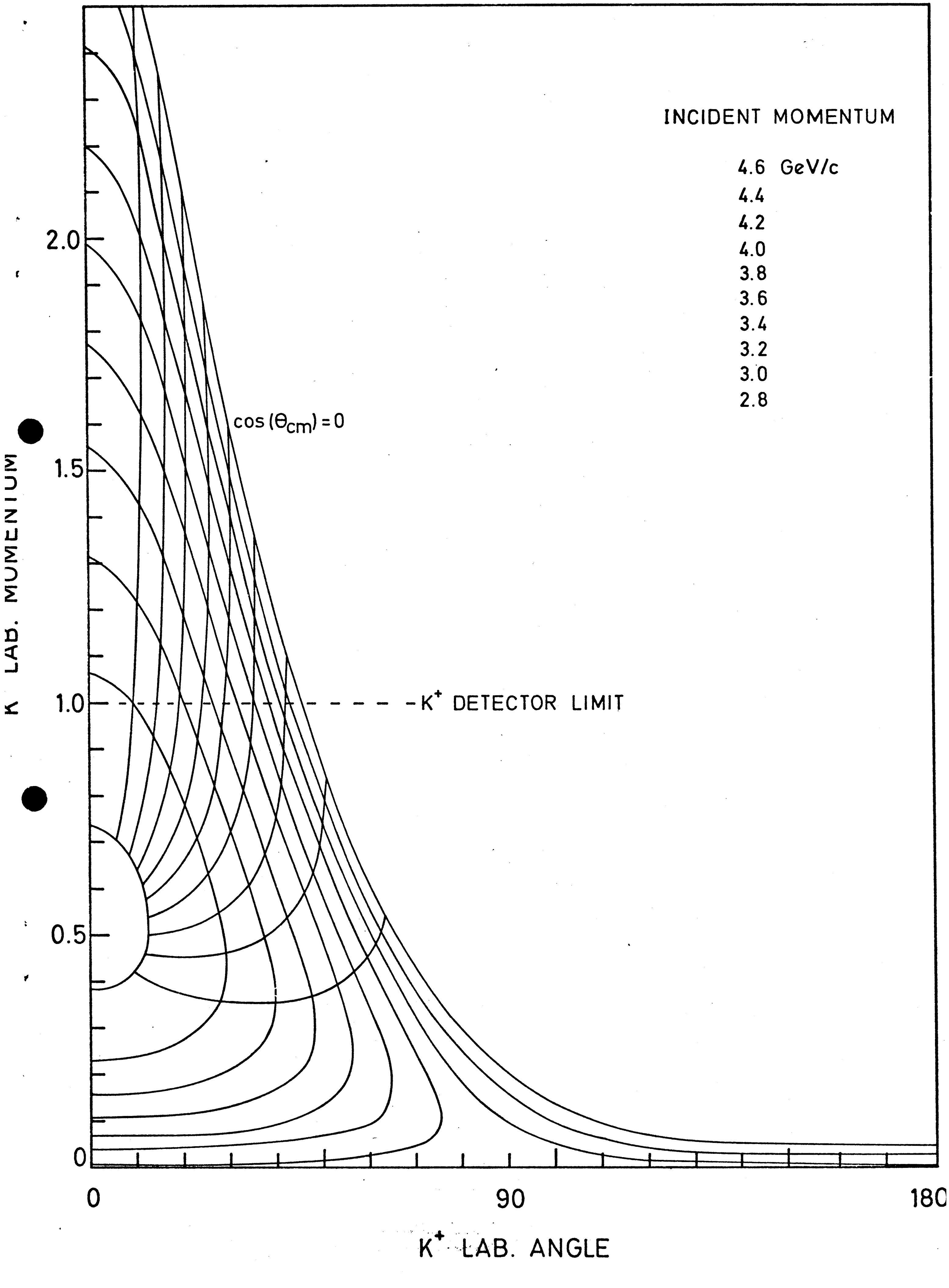

Figure 4 ACCEPTANCE OF K DETECTORS VERSUS INCIDENT MOMENTUM FOR THE REACTION $K^- + P \longrightarrow K^+ + \Xi(2030)$